



# Uncertainty quantification in inerter-based quasiperiodic lattices

Tanmoy Chatterjee<sup>a,b</sup>, Danilo Karličić<sup>c,\*</sup>, Milan Cajić<sup>b,c,\*\*</sup>, Sondipon Adhikari<sup>d</sup>, Michael I. Friswell<sup>b</sup>

<sup>a</sup> School of Mechanical Engineering Sciences, University of Surrey, Guildford GU2 7XH, UK

<sup>b</sup> Faculty of Science and Engineering, Swansea University, Swansea SA1 8EN, UK

<sup>c</sup> Mathematical Institute of the Serbian Academy of Sciences and Arts, 11000 Belgrade, Serbia

<sup>d</sup> James Watt School of Engineering, The University of Glasgow, Glasgow G12 8QQ, UK

## ARTICLE INFO

### Keywords:

Quasiperiodic lattices  
Uncertainty quantification  
Acoustic metamaterials  
Gaussian process  
Hofstadter's butterfly  
Edge states

## ABSTRACT

Inerter-based periodic structures have attracted significant interest among the research community due to their wide range of applications. However, existing studies on quasiperiodic structures, especially with inerters, are limited. Therefore, this timely work investigates the dynamics of novel one-dimensional inerter-based quasiperiodic lattices with and without local resonators. The quasiperiodicity is introduced through the modulation of both spring and inerter properties resulting in the well-known Hofstadter-like butterfly spectrum having a fractal structure. Moreover, by considering the appropriate boundary conditions and many mass-spring-inerter subsystems, the bulk spectrum of the system is investigated demonstrating the existence of multiple edge states in lower and higher frequency ranges. The deterministic study showed that the effect of inertia amplification is to reduce the frequencies of the Hofstadter-like butterfly and to widen the low frequency band gaps. The second contribution of this work involves investigating the effect of parametric uncertainty for the acoustic-metamaterial-like chain based on Monte Carlo simulations. Moreover, to address the computational aspect of the problem, grey-box modeling using machine learning was performed. A Gaussian process model was trained on a limited dataset and was found to capture the stochastic responses of the lattices adequately. The statistical variation of parameters with different levels of uncertainty demonstrated significant effects on the Hofstadter-like butterfly, band gaps, corresponding edge states and frequency responses. The sensitivity of the dynamic behavior in quasiperiodic lattices to variabilities reveal the need to account for system uncertainties for their targeted performance as future vibration absorbers and energy harvesters. The study also paves the way to utilize the results as useful prior information for robust design optimization of real inerter-based quasiperiodic lattice devices.

## 1. Introduction

The design of periodic structures has been exploited in different ways to gain unique wave propagation characteristics and topological phenomena in metamaterials and metastructures. In recent years, special attention was devoted to mechanical metamaterials that exhibit topologically protected edge and interface modes which are robust to defects/disorder and uncertainties in the periodical arrangement of the materials [1,2]. This field emerged from condensed matter physics, where topological insulators [3] have attracted significant attention of the metamaterials community due to potential applications in wave localization and transport [4–6]. Consequently, the underlying physics was widely utilized in classical wave-supporting materials to emulate the edge states. This includes simple 1D lattices based on the Su-Schrieffer-Heeger model [7] and 2D lattices with effects analogous to

quantum Hall phases [8–11], where localized edge states exist at an interface separating two distinct topological phases [12–14]. Robust elastic wave topological edge modes were realized and proved to exist in mechanical metamaterials and phononic lattices, including linear locally resonant [15,16] and nonlinear lattice systems [17–21].

Some recent studies exploited the Aubry-André model [22] to modulate 1D quasiperiodic linear [23] and nonlinear [24] lattices that form Hofstadter-like spectra with similar topological gaps and edge states to those which occur in 2D electronic lattices as a consequence of the quantum Hall effect. Moreover, in [23] it was found that every band gap in the bulk resonant spectrum of a quasiperiodically coupled discrete mechanical resonator is topological. This was proven by using the arguments from the  $K$ -theory developed in [25]. Later, the same

\* Corresponding author.

\*\* Corresponding author at: Faculty of Science and Engineering, Swansea University, Swansea SA1 8EN, UK.

E-mail addresses: [danielok@mi.sanu.ac.rs](mailto:danielok@mi.sanu.ac.rs) (D. Karličić), [milan.cajic@swansea.ac.uk](mailto:milan.cajic@swansea.ac.uk), [mcajic@mi.sanu.ac.rs](mailto:mcajic@mi.sanu.ac.rs) (M. Cajić).

principles were used in [26] for sound waves in quasiperiodic acoustic waveguides, where in contrast to the previous studies, a continuum medium treatment of the lattice was employed along with the Chern number defined on the three-dimensional noncommutative manifold and used to assess the topological character of the gaps. In [27], the authors studied the Hofstadter butterfly and the emergence of topological edge states in reconfigurable quasi-periodic acoustic crystals. Moreover, gaps are uniquely labeled by the value of integrated density states (IDS) inside the gaps while the Hofstadter butterfly spectrum was mapped through the acoustic density of states (DOS). The experimental and theoretical observation of a metastructure that constitutes a beam with quasiperiodically placed local resonators was performed in [28]. Investigation of the dynamic behavior and topology of the proposed metastructure revealed the existence of additional topologically non-trivial band gaps with associated edge-localized modes that occur due to the quasiperiodical arrangement of resonators. This means that quasiperiodic metastructures with local resonators can generate wave localization and attenuation over multiple frequency bands and potentially be used in energy harvesting and vibration isolation applications. Moreover, in [29] the authors explored the 1D quasiperiodic metastructure having modulated LEGO resonators, i.e. modulation is performed by sliding the cones along the pillars, thus showing its potential for simple aperiodic patterning of local resonances and observation of topological phenomena. The Hofstadter-like resonant spectrum was mapped and non-trivial spectral gaps identified through the numerical and experimental investigations. Some authors extended the wave propagation analysis to two-dimensional elastic quasicrystalline metamaterials and composites [30,31] exhibiting 8-, 10- and 14-fold rotational symmetries.

Inerters as separate elements in mechanical systems have been widely investigated in recent years [32]. Practical inverter devices have been realized in different manners [33] including fluid-based inerters [34] and mechanical flywheel inerters based on gear or ball-screw mechanisms [35]. Their application often includes, but it is not limited to, passive vibration absorption. Recently, an acoustic metamaterial with a unique sound pressure amplification mechanism that is analogous to a mechanical inverter was used for ultra-low frequency sound attenuation [36]. Other studies analyzed the effect of inerters on wave propagation in acoustic [37], seismic [38] and locally resonant metamaterials [39,40]. In [41], the authors suggested an architecture of inertial metamaterials to design mechanical lattices with novel topological and dispersion properties, where stable negative inertial coupling is used as the key mechanism to achieve certain topological classes. In this work, we use, for the first time, quasiperiodically modulated inerters within the broader setup of 1D quasiperiodic lattices and investigate its bulk spectra and edge states.

Although significant work has been done in the field of periodic mechanical metamaterials and metastructures with inverter elements, little has been done on the quasiperiodic analog of such systems, especially with inerters. Moreover, defects and anomalies in periodicity are common in manufacturing of engineering metamaterials, posing problems for the targeted control of acoustic and elastic waves and lead to deviations of the predicted dispersion properties based on simple theoretical models [42]. The problem of one-dimensional [43] and two-dimensional [44] elastic metamaterials with geometric and material uncertainties was addressed to quantify their effect on the dispersion characteristics of the system.

In the present work, we consider one-dimensional quasiperiodic mass-spring-inverter chains and investigate their dynamical behavior in the presence of system uncertainties. To the best of the authors' knowledge, the deterministic and stochastic analysis of quasiperiodic arrangements of mass-spring-inverter lattices has not been considered in the literature. Moreover, since quasiperiodic lattices have a chain-like configuration connecting multiple elements, this can easily lead to large-sized system matrices upon assembly. Therefore, the computational aspect of the framework was also investigated by posing the

problem as supervised learning and constructing a grey-box model using a machine learning technique, namely a Gaussian process. In particular, the emphasis here is placed on the investigation of the effect of parametric uncertainty on the Hofstadter-like butterfly and the frequency response function. To better understand the impact of inerters and uncertainty on quasiperiodic discrete lattices, two different cases with and without local resonances are considered. Moreover, the presence of edge-localized modes within the nontrivial band gaps is studied based on the finite-lattice spectrum for the deterministic case.

## 2. The inverter-based quasiperiodic lattices

The band structure properties of classical mechanical metamaterials and periodic lattices are well-known and widely investigated in the literature. The expected behavior of such systems includes the appearance of stop (band gaps) and pass bands that enable them to work as filters and isolators for propagating waves at certain frequency ranges. The recent introduction of inerters into periodic lattices [45] demonstrated their remarkable tuning properties and impact on band structure, where the frequency of bands, corresponding gaps, and even topological interface modes was shifted to lower values. A similar influence of inerters is expected in 1D quasiperiodic lattices as well, with the main difference that quasiperiodicity will result in interesting Hofstadter butterfly and edge mode spectra. Therefore, in this section, we present a short introduction to mechanical inverter devices and their possible physical realizations. This will be followed by theoretical foundations of inverter-based quasiperiodic lattices and formation of the eigenvalue problem.

### 2.1. Preliminaries to inerters

Smith [46] suggested a mechanical analog of the equivalent electrical network and proposed several different configurations of the mechanical inerters. Since this seminal work, various types of inerters have been developed (e.g. see Fig. 1(a)) and widely accepted as tunable vibration isolation devices [47]. A similar analogy was used in [36] to realize an acoustic inverter, where a unique sound pressure amplification mechanism was used for ultra-low frequency noise control. A different mechanism was used in [48] with an inertial force generated by moving fluid mass.

In general, inverter is considered as a two-terminal mechanical device whose force is proportional to the relative acceleration between the two terminals with the force given as

$$F = b (\ddot{u}_2 - \ddot{u}_1) \quad (1)$$

where  $b$  is the inertance parameter,  $\ddot{u}_1$  and  $\ddot{u}_2$  are the accelerations of the terminals and  $F$  is the force acting on the inverter. More complex relations for the inverter's force have been obtained and confirmed experimentally [35] for fluid-based inerters.

A metamaterial beam with periodically distributed inverter-based local resonators given in the form of mechanical networks was studied in [49]. Thus, ideal inerters can be used in different combinations with springs and viscous dampers to form mechanical networks (e.g. see Fig. 1(b)). Although the behavior of real mechanical inerters cannot be described by a simple relation, such as that of the ideal inverter, it can give us insight into the effects of inertia amplification in both simple mechanical systems as well as in periodic systems. In recent work by Van Damme et al. [50], an inertial amplification factor of  $\alpha = 1/\sin^2 \theta_0$  was obtained under the assumption of small strains for one degree of freedom system with mechanical inverter similar to that in Fig. 1(a) but having a non-linear damping term. It should be noted that in our work, by using the assumption of small strain, we have employed the ideal inverter elements with modulated properties within a broader setup of quasiperiodic chains. The aim of the following analysis is to reveal the effect of inertia amplification on the Hofstadter butterfly spectra and edge states.

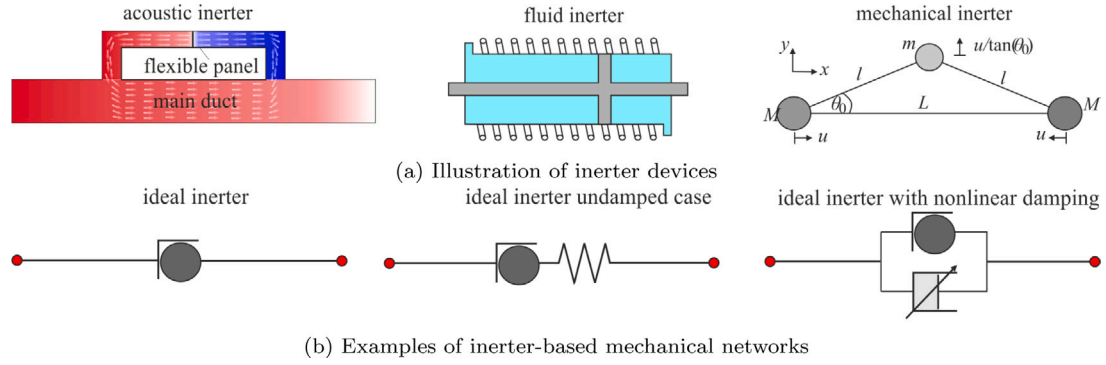


Fig. 1. Illustration of different physical realization of inerter devices available in the literature (e.g. see [36,48]) and discrete models of mechanical networks [49].

## 2.2. Problem formulation

In the previous discussion, we mentioned how mechanical inerters can be used in periodic metamaterial lattices to achieve inertia amplification and obtain unique dispersion properties. Al Ba'ba'a et al. [41] proposed a physical model of a monoatomic chain based on mechanical inerters and discovered interesting dispersion and topological properties of such artificially architected lattices. The authors employed an ideal inerter model with the simplified linearized relationship for the equivalent inertial coupling, where the effect of positive and negative angles of the inerter's slider on stability was also addressed. Here, we also suggest a possible configuration for the physical realization of the locally resonant quasiperiodic acoustic-metamaterial-like chain with mechanical inerters (see Fig. 2 a). Having in mind that inerters are tunable devices [51], the quasiperiodicity can be achieved by modulating both stiffness and inertia properties. However, for the purpose of this theoretical investigation, we will assume an idealized discrete mass-spring-inerter chain model as given in Fig. 2 (b) and (c). Here, we will observe only a large super-cell of the chain but not in the sense of Bloch analysis, which is sometimes difficult to perform on large unit cells, but rather by imposing the periodic boundary conditions such that it geometrically resembles a ring [28]. Two different lattice configurations will be studied including the phononic-crystal-like (PCL) chain (Fig. 2 b) and the locally resonant acoustic-metamaterial-like (AML) chain (Fig. 2 c). Therefore, the super-cell is constituted of many smaller mass-spring-inerter-based unit cells (subsystems) in the case of PCL chain or mass-in-mass subsystems connected through spring-inerter elements in the case of AML chain.

The general form of governing equations of the mass-spring-inerter lattice system (the case with local resonators) with modulated stiffness and inerter properties can be expressed as

$$M_r \ddot{u}_r^n + k_{r-1}(u_r^n - u_{r-1}^n) + k_r(u_r^n - u_{r+1}^n) + k_{gr} u_r^n + k_{Rr}(u_r^n - v_r^n) + \quad (2)$$

$$B_{r-1}(\ddot{u}_r^n - \ddot{u}_{r-1}^n) + B_r(\ddot{u}_r^n - \ddot{u}_{r+1}^n) + B_{gr} \ddot{u}_r^n = 0,$$

$$m_r \ddot{v}_r^n + k_{Rr}(v_r^n - u_r^n) = 0, \quad (3)$$

where  $r = 1, \dots, R$ ,  $R$  is the number of masses in the super-cell with a sufficiently large number of subsystems while superscript  $n$  represents the number of a super-cell in the chain and can be neglected in the further analysis since only a single super-cell will be considered. The governing equations for the case without local resonators can be easily recovered by setting the stiffness  $k_{Rr}$  of the local resonator in Eq. (2) equal to zero (Eq. (3) is neglected).

The quasiperiodicity is introduced through modulated stiffness and inerter coefficients according to the following law

$$k_r = k_0(1 + \beta_m \Gamma_r) = k_0 C_r, \quad (4)$$

$$k_{gr} = k_0 \gamma_g(1 + \beta_{gm} \Gamma_r) = k_0 \gamma_g D_r,$$

$$k_{Rr} = k_0 \xi_R(1 + \theta_m \Gamma_r) = k_0 \xi_R G_r,$$

$$B_r = sM(1 + \rho_m \Gamma_r) = sM V_r, \quad B_{gr} = \epsilon_g M(1 + \rho_{gm} \Gamma_r) = \epsilon_g M W_r, \quad (5)$$

$$M_r = M(1 + \delta \Gamma_r) = M H_r, \quad m_r = bM(1 + g \Gamma_r) = bM J_r, \quad (6)$$

where  $\Gamma_r = \cos(r\theta + \phi)$ ,  $r = 1, 2, \dots, R$ . The parameter  $\theta$  is the one that controls the periodicity of the modulation (it can have rational or irrational values related to periodic and quasiperiodic domains, respectively) while the phase  $\phi$  does not affect the periodicity but it is important for the existence of edge states at the boundaries (e.g. see [29]). The relation between the masses of the outer and inner elements in the unit cell is given as,  $b = m/M$ .

Our aim is to compute eigenfrequencies that represent the spectrum of the bulk and corresponding infinite domains. Now, the system of Eqs. (2) and Eq. (3) can be given in matrix form for the super-cell with many mass-spring-inerter subsystems (and local resonators) as

$$\frac{1}{\omega_0^2} \mathbf{M} \ddot{\mathbf{u}}_n + \mathbf{K} \mathbf{u}_n + \frac{1}{\omega_0^2} \mathbf{M}^{(l)} \ddot{\mathbf{u}}_{n-1} + \mathbf{K}^{(l)} \mathbf{u}_{n-1} + \frac{1}{\omega_0^2} \mathbf{M}^{(r)} \ddot{\mathbf{u}}_{n+1} + \mathbf{K}^{(r)} \mathbf{u}_{n+1} = \mathbf{0}, \quad (7)$$

where  $\mathbf{M}$  and  $\mathbf{K}$  are the corresponding mass and stiffness matrices, respectively, while  $\mathbf{u}_n$  is the vector of displacements (the natural frequency of a single oscillator is given as  $\omega_0^2 = k_0/M$ ). Further, we employ periodic boundary conditions on both ends of the chain so that it geometrically represents the ring. In that respect, the left and right interactions of the mass and stiffness matrices are expressed as  $\mathbf{M}^{(l)}$ ,  $\mathbf{K}^{(l)}$ , and  $\mathbf{M}^{(r)}$ ,  $\mathbf{K}^{(r)}$ .

As given in [52], the modes of the ring-like chain coincide with the Bloch modes. Therefore, the procedure similar to those applied in [52] can be used to form the eigenvalue problem in our case, which gives

$$(\tilde{\mathbf{K}} - \Omega^2 \tilde{\mathbf{M}}) \mathbf{a} = \mathbf{0}, \quad (8)$$

where  $\mathbf{a}$  is the eigenvector and  $\mathbf{K}(\mu)$  and  $\mathbf{M}(\mu)$  are wavenumber dependent stiffness and mass matrices, respectively, given as

$$\tilde{\mathbf{M}}(\mu) = \mathbf{M} + \mathbf{M}^{(l)} e^{i\mu} + \mathbf{M}^{(r)} e^{-i\mu}, \quad (9)$$

$$\tilde{\mathbf{K}}(\mu) = \mathbf{K} + \mathbf{K}^{(l)} e^{i\mu} + \mathbf{K}^{(r)} e^{-i\mu}.$$

## 3. Hofstadter butterfly and edge states: Deterministic case

In physics, the Hofstadter butterfly effect refers to a complex fractal pattern of energy states of electrons i.e., energy spectrum that describes the behavior of electrons in a magnetic field. Recently, a Hofstadter-like

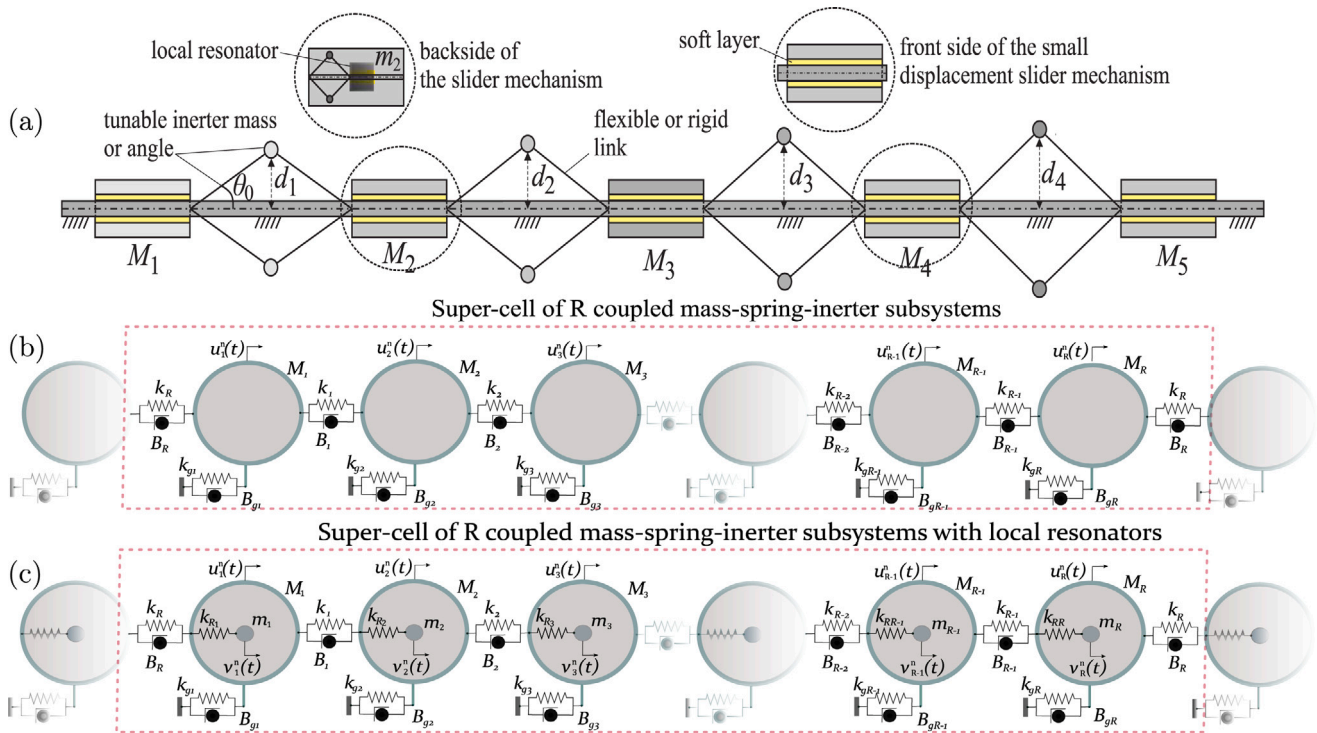


Fig. 2. The inerter-based 1D quasiperiodic lattices consisting of mass–spring–inertersubsystems: (a) possible physical realization of the lattice, and idealized mechanical models of (b) phononic-crystal-like chain (c) locally resonant acoustic-metamaterial-like chain.

butterfly pattern and interesting edge states were noticed in classical wave dynamics systems given as quasiperiodic locally resonant metastructures [28]. Such analysis can give us an insight into how the quasiperiodicity affects the existing band gaps and associated edge-localized states only through the variation of mechanical parameters of the system. An additional challenge is to investigate the effect of inerters, as pure mechanical devices, on such generated gaps and edge states. Therefore, in this section, we perform deterministic analysis to examine the influence of inertia amplification parameter on the Hofstadter-like butterfly and edge states spectrum of 1D quasiperiodic lattices. To observe this in our case, we adopt a sufficiently large number of mass–spring–inertersub-unit cells in the case of the 1D phononic-crystal-like (PCL) quasiperiodic chain and the corresponding number of local resonators in the case of the acoustic-metamaterial-like (AML) quasiperiodic chain. For this purpose, we adopt  $R = 200$  masses with the same number of degrees of freedom in the unit cell of the PCL chain, whereas that number is doubled in the case of the AML chain due to the local resonators. Moreover, we observe the bulk spectra in terms of phase  $\phi$  to show the edge states crossing the gaps and demonstrate their localization at boundaries. However, it is to be noted that the aim of this study is not to prove the non-trivial topological nature of the band gaps (by investigating topological invariants) but to investigate the effect of parametric uncertainty on the Hofstadter butterfly and bulk spectra of the mass–spring–inertersubsystems. This section is also expected to help in visually distinguishing the subtle differences of the resulting Hofstadter butterfly spectrum behavior without and in the presence of system uncertainties.

First, we map the Hofstadter butterfly spectrum for the case of the following deterministic system parameters of the AML chain, if not given otherwise:  $\beta_m = 0.15$ ,  $\gamma_g = 1$ ,  $b = 0.1$ ,  $\beta_{gm} = 1$ ,  $\xi_R = 0.08$ ,  $\theta_m = 0.5$ ,  $g = 0.2$ ,  $s = 0.1$ ,  $\rho_m = 0.1$ ,  $\rho_{gm} = 0.13$ ,  $\epsilon_g = 0.2$ ,  $\epsilon_g = 0.2$  and  $\delta = 0.1$ . The same values of parameters are used for the PCL chain where only the stiffness of the local resonator is neglected. In both cases, the periodic boundary conditions (to form the ring-like structure) are used at the ends of the super-cell of the chain.

Fig. 3 shows how the frequencies of the AML and PCL quasiperiodic chains vary in terms of the quasiperiodic parameter  $\theta$  resulting in the fractal structure similar to the Hofstadter butterfly. The resonant frequencies of the system discretize the bulk spectrum whose density directly depends on the number of considered masses. One can observe a large zero-frequency gap, whose existence is attributed to the ground springs, and a number of additional gaps inside the butterfly-like spectrum. Moreover, the differences in the Hofstadter butterfly for configurations with and without inerter elements can be viewed from Fig. 3(a) and Fig. 3(b) for the quasiperiodic AML chain and Fig. 3(c) and Fig. 3(d) for the PCL chain. The introduction of inerter elements into the chain significantly shifts the Hofstadter butterfly spectrum to lower frequencies but at the same time keeps almost the same fractal structure in the quasiperiodic PCL chain. The frequency shifting is much more pronounced in the higher frequency range than in the lower one. However, the major difference can be noticed in the quasiperiodic inerter-based AML chain, where the lower frequency gaps associated with the local resonances are notably larger than those in the configuration without inerters. The significance of this feature of inerter-based quasiperiodic chains will be additionally discussed in the following part of this section. To predict the existence of edge states and the non-trivial nature of gaps emerging within the Hofstadter butterfly spectrum, some authors [28] suggested estimation of the integral density of states (IDS). The variation of IDS with  $\theta$  can give us important information such as the number of band gaps and topological boundary modes spanning those gaps between two subsequent commensurate values of  $\theta$ . However, as we stated previously, this analysis is out of the scope of this study and the main focus will be on the investigation of the effect of parametric uncertainty on the dynamics of PCL and AML chains with quasiperiodic patterns.

For the purpose of identifying the edge states we calculate the bulk and edge state spectra for finite lattices as a function of the phase  $\phi$  and for the fixed value of  $\theta = 0.2 \cdot (2\pi)$ . In this case, free-free boundary conditions are used to achieve and demonstrate the existence of edge-localized states. Fig. 4 shows the bulk spectra of the AML and PCL chains with edge states crossing both higher and lower frequency gaps.

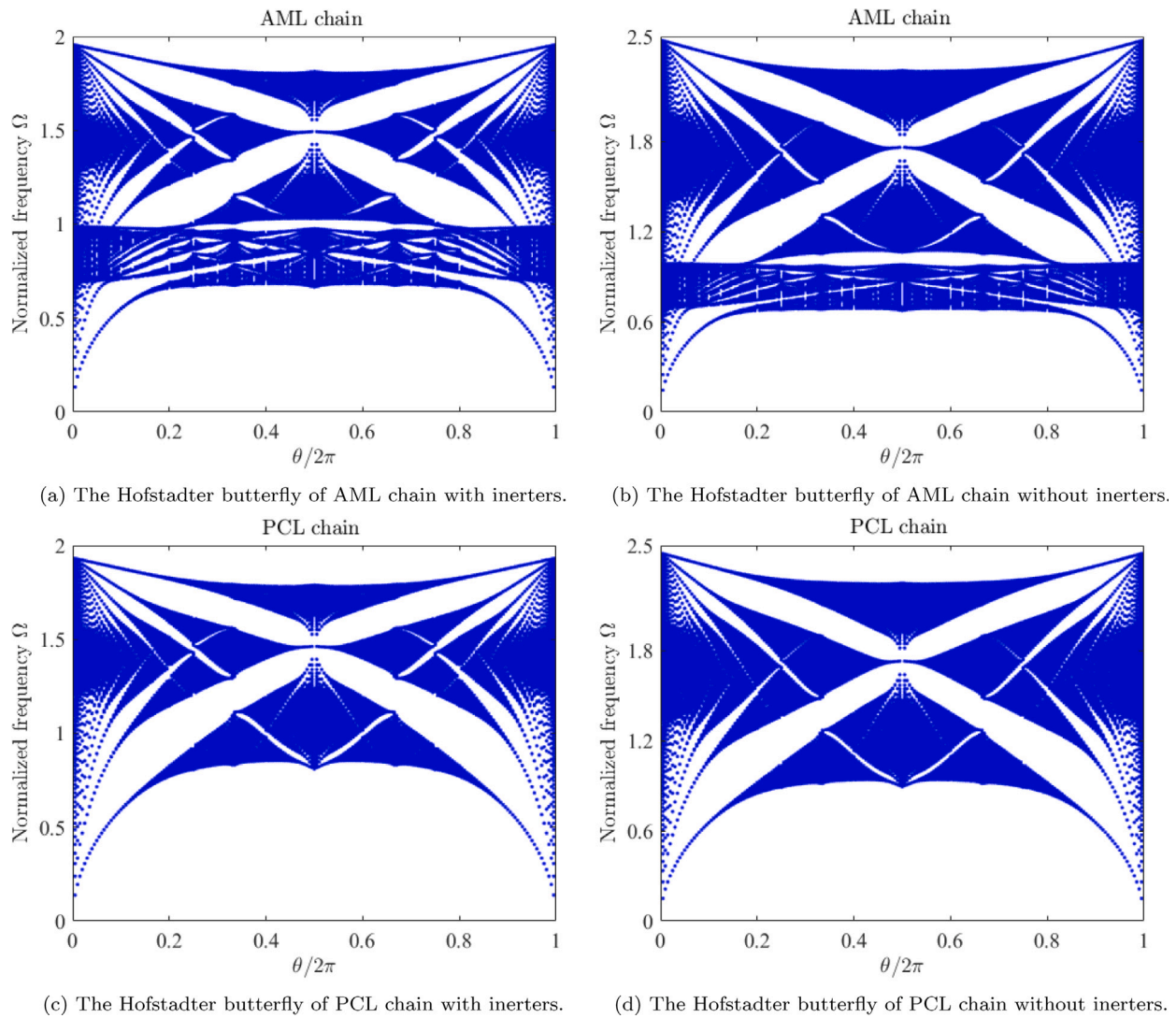


**Fig. 3.** The Hofstadter butterfly of quasiperiodic AML and PCL chains with and without inerter elements and nominal (deterministic) system parameters. The case with ground and intermass inerter is given for  $\epsilon_g = 0.2$  and  $s = 0.1$ .

The number of crossings that are related to left or right-end localization in the chain is different for each of the gaps and can be one or two. This number is directly dependent on the topological features of the gap which can be found by determining the Chern numbers (that can be computationally expensive for large cells) or estimation of IDS. However, that analysis is not performed in this study due to the reasons mentioned previously. The spectrum of the AML chain demonstrates the existence of multiple small gaps crossed with edge states and located in the lower frequency region owing to the local resonance nature. Those low-frequency gaps are missing in the PCL chain, where the first large gap (apart from the existing zero-frequency gap) appears around the unit frequency crossed with two edge states. Similar large gaps appear in the higher frequency ranges of the AML chain. The mode localization shown for the edge states from these large gaps in Fig. 4(b) and Fig. 4(d) demonstrates localization at both ends of the chains. However, the chosen eigenstates from the spectrum show no localization in both the AML or PCL chains.

To reveal the effect of inerter on the bulk spectra and edge states, a comparison of the case without and with inerter for the quasiperiodic AML and PCL chains is presented in Fig. 5. It is expected that the frequencies will reduce due to the mass amplification effect. Therefore, Fig. 5(a) shows the spectrum of the AML chain that is shifting along with the band gaps and corresponding edge states towards lower

frequency values when ground and inter-mass inerter are introduced. Similar behavior can be noticed in the PCL chain with inerter. It should be emphasized that this shifting of band gaps along with the edge states is much more pronounced at higher frequency ranges, which is consistent with the effect of inerter noticed in some previous works [45]. One important property of quasiperiodic AML chains is the generation of multiple lower-frequency band gaps (crossed with corresponding edge states) that are associated with local resonances. However, a significant flattening and widening of the low-frequency band gaps in their narrowest part can be observed in the configuration with inerter elements, which is also followed by the separation of edge states from the bulk. However, the shape of these low-frequency gaps strongly depends on the phase  $\phi$  in both configurations with and without inerter. Similar behavior of inerter was noticed earlier in the literature [40,53], where widening of low-frequency gaps was noticed even for small mass fractions in inertia amplifiers [53], which would require much larger resonant masses in the pure locally resonant periodic structures.

#### 4. Hofstadter butterfly and edge states: Stochastic case

In this section, a numerical study has been conducted to quantify the variation of the dynamic behavior of inerter-based quasi-periodic

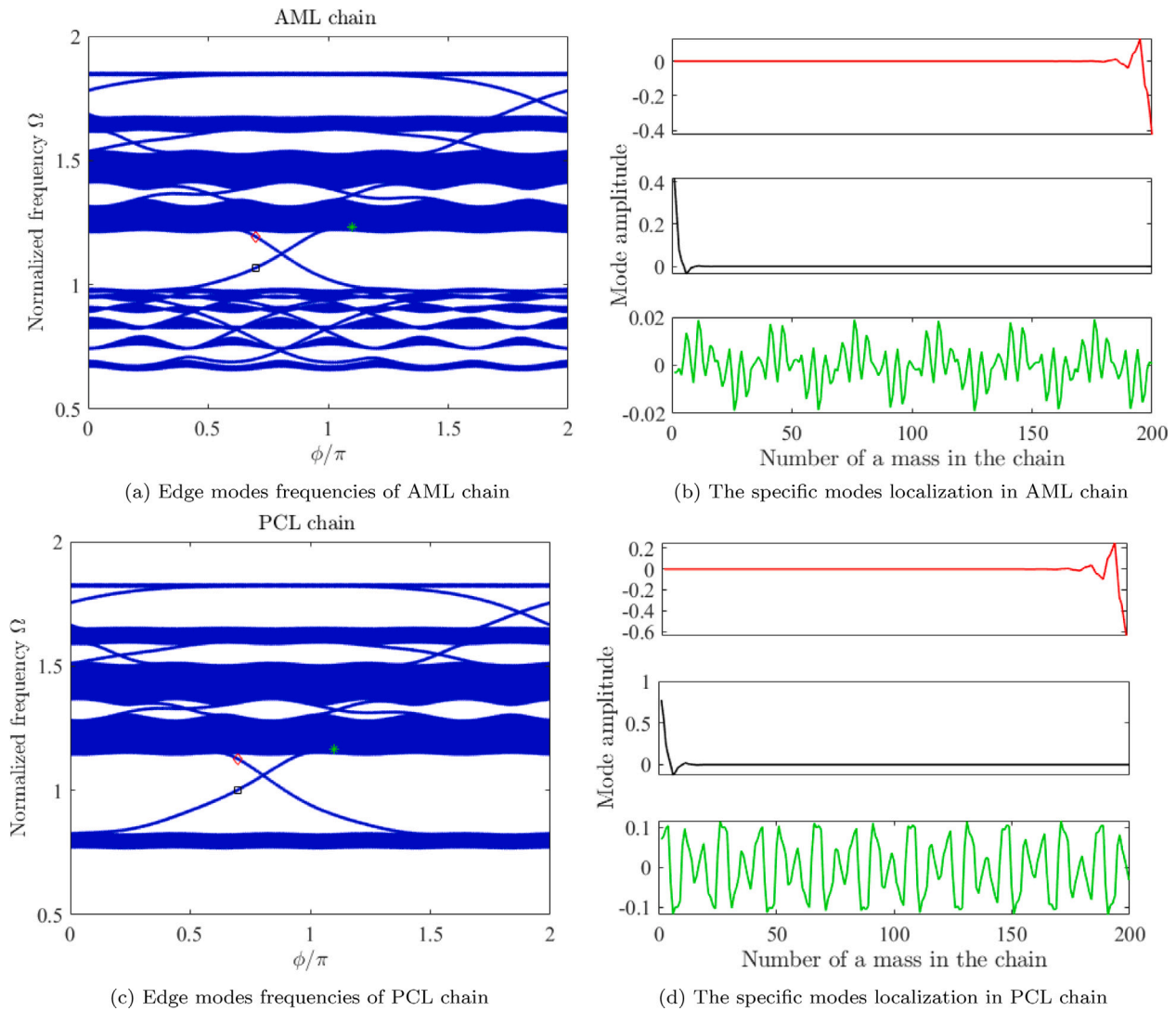


**Fig. 4.** The bulk spectra and edge states in quasiperiodic AML (a) and PCL (c) chains for varying phase  $\phi$  and  $\theta = 0.2 \cdot (2\pi)$ . The  $R = 200$  masses is considered in PCL chain and the same number of resonators in AML chain. The particular values from the bulk and edge mode spectra of AML chain are chosen from panel (a) and from panel (c) for PCL chain and their localization given in panels (b) and (d), respectively.

lattices considering multiple sources of uncertainties. Although insightful and interesting results were obtained for the PCL lattice in the deterministic case study, for the stochastic analysis, we restrict ourselves to the more complex case of the AML lattice. Uncertainties in material, geometry, and loading are inevitable in engineering practice. Thus, carrying out stochastic analysis in the pre-design stage could be a key step to ensure the desired performance of quasiperiodic lattices and detect any significant deviation which may prove to be detrimental.

In recent years, Gaussian process (GP) models have received considerable attention in the scientific and engineering community. The history of GP in geostatistics traces back to the last century but their capability to solve complex engineering problems has immensely contributed to their success trajectory. More theoretical details on GP can be found in [Appendix](#) and the references within. Here, we first determine the optimal number of sample points to train the GP model to approximate the dispersion behavior and frequency responses, where error convergence studies have been performed as shown in [Fig. 10](#) in [Appendix](#). The same values of parameters that are used in the previous deterministic study are also employed here as nominal values for the following stochastic analysis.

The statistical variation in the dispersion behavior due to 10% uncertainty in the mass, stiffness and inerter parameters has been

presented in [Fig. 6](#). The performance of GP to capture the variation in the dispersion behavior has been compared with Monte Carlo simulation (MCS). The maximum, mean and minimum responses are presented to illustrate the response variation. As expected, the mean response is close to the response of the nominal (deterministic) case, where a similar fractal structure of the Hofstadter butterfly spectrum and corresponding band gaps can be observed. Further, the maximum response displays shifting of butterfly to larger frequencies having wider gaps (especially in the lower frequency region), which can be attributed to increased stiffness, local resonance masses and inertia effects. On the other side, the minimum response shifts the butterfly to lower frequency values displaying much narrower gaps in the lower frequency region that might be attributed to lower values of stiffness, local resonance masses and inertia amplification.

It can be observed from the results in [Fig. 6](#) that the GP model trained with 50 samples has approximated the dispersion statistics accurately. This is worth noting considering the fact that the dispersion behavior exhibits nonlinear fluctuations and sudden opening and closure of stop bands. However, it should be noted that the GP model fails to predict some of the lower frequency states as compared to MCS, which can be improved by increasing the number of training samples.

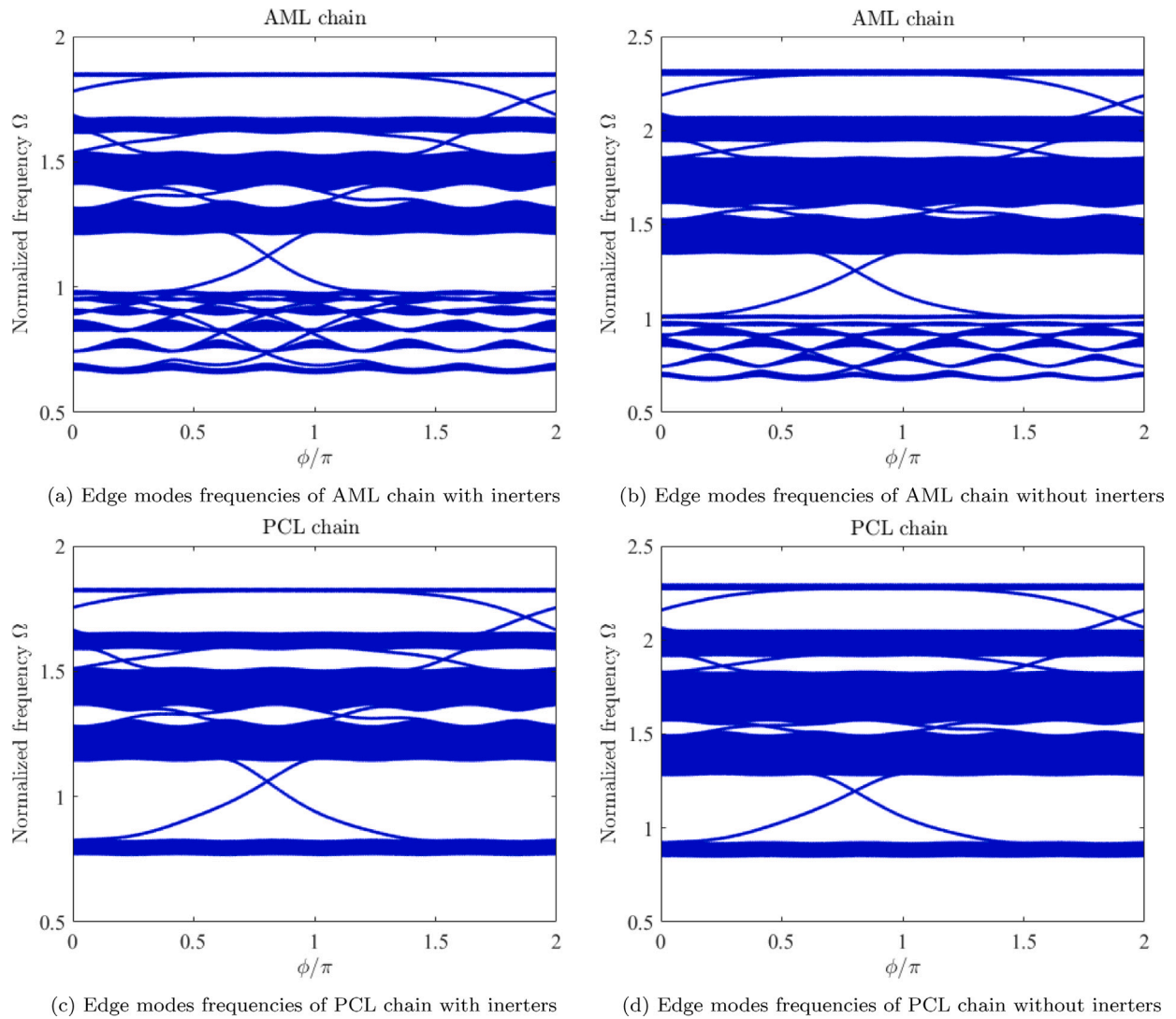


**Fig. 5.** The bulk spectra and edge states of quasiperiodic AML and PCL chains for varying phase  $\phi$  and  $\theta = 0.2 \cdot (2\pi)$  given in the configurations with and without inerter elements when  $s = 0.1$  and  $\epsilon_s = 0.2$ .

As negligible changes were observed in the mean dispersion response due to varying levels of uncertainties, only the extreme (maximum and minimum) values were plotted in Fig. 7 to illustrate the significant changes in the dispersion trends with varying levels of uncertainties. Therefore, the effect of varying levels of uncertainties (10%–20%) in the mass, stiffness, and inerter parameters has been studied. By comparing the maximum butterfly spectrum responses for 10% and 15% uncertainty shows a slight shifting of the spectrum to higher frequency values but no significant changes in the fractal structure of the spectrum can be noticed. A similar observation can be viewed in the case of 20% uncertainty where the additional shifting of the Hofstadter butterfly spectrum to higher frequencies is present. Slightly different conclusions can be drawn for the minimum responses where the major change occurs in the low-frequency region where the fractal structure of some of the gaps is changed and the lowest modes are strongly affected by the increased level of uncertainty. Although the investigation is not presented here, the parameter that contributes the most to the migration of low-frequency modes to zero is the parameter that modulates the ground inerter properties. Moreover, a slight shifting of the whole spectrum to lower frequency values can also be observed.

The stochastic bulk spectra and edge states of the AML chain due to 10% uncertainty in the mass, stiffness, and inerter parameters

have been presented in Fig. 8. This analysis is performed to show the effect of parametric uncertainty on edge states of the AML chain since this property cannot be investigated from the Hofstadter butterfly. The mean, minimum and maximum of the bulk spectra stochastic responses are given as a function of the phase  $\phi$  and for a fixed value of  $\theta = 0.2 \cdot (2\pi)$ . The mean response is the one that resembles the deterministic case as discussed in the previous section. On the other side, the maximum response demonstrates a significant shifting of the bulk spectra to higher frequencies with a slight widening of the band gaps crossed with the same number of edge states as for the mean case. However, a significant change in the bulk spectra properties can be observed in the minimum response. These changes are notable in the low-frequency band gaps that are related to local resonances, where a significant narrowing and widening of gaps occur for certain values of phase followed by the migration of edge states towards the bulk. Moreover, the narrowing of the higher frequency gaps can be observed in the minimum response.

The frequency response function (FRF) statistics due to 10%, 15% and 20% uncertainty in the mass, stiffness, and inerter parameters are presented in Fig. 9. The performance of the GP trained with 100 samples for 10% uncertainty has also been compared with that of MCS demonstrating accurate capturing of the FRF statistics. The FRFs are evaluated assuming 0.5% damping. The comparison of the

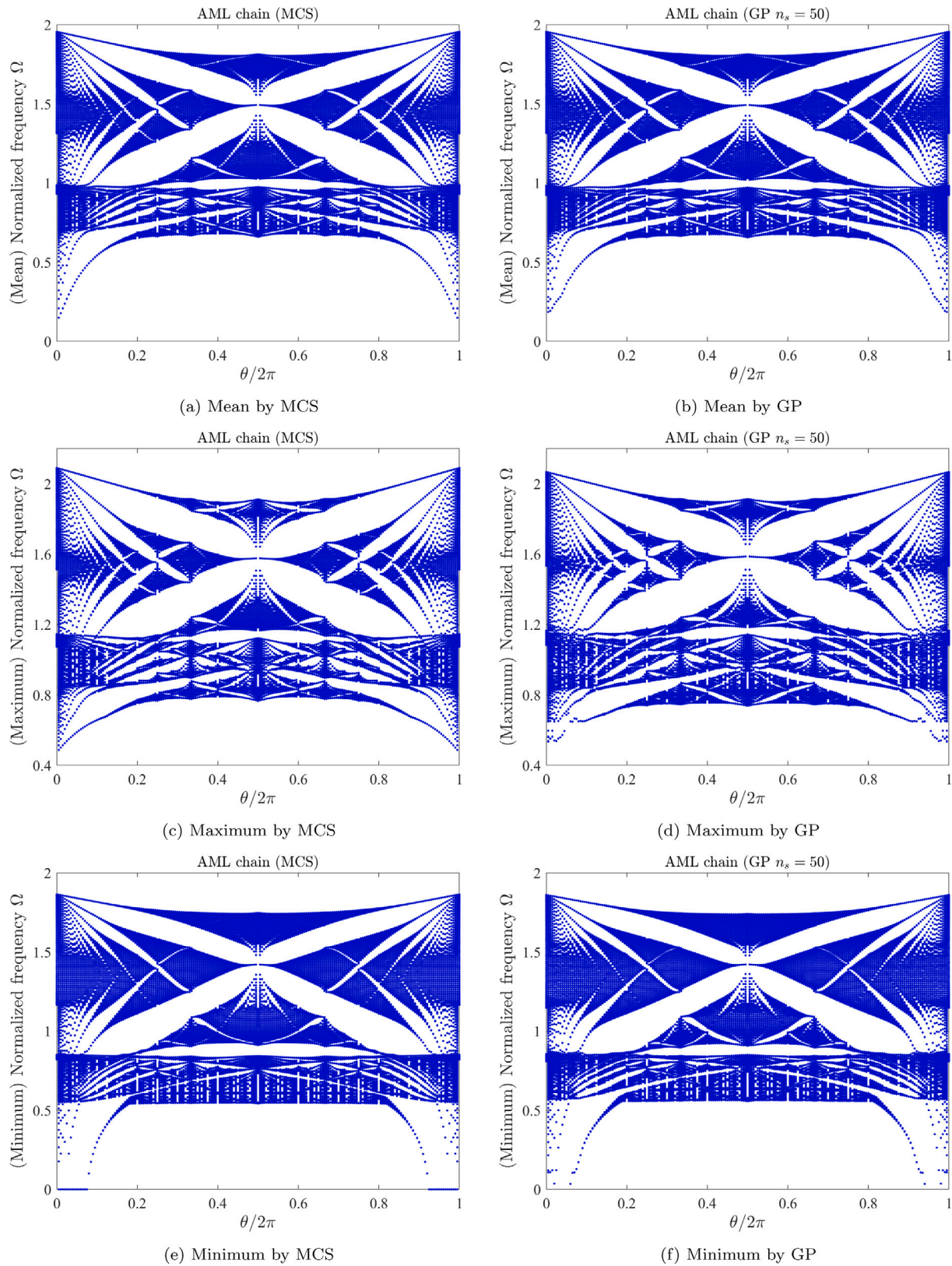


**Fig. 6.** Comparison of the performance of GP (right) with that of MCS (left) in capturing the statistics of the Hofstadter butterfly spectrum behavior in the presence of 10% uncertainty. 50 samples have been employed to train the GP model.

ensemble mean and deterministic case shows significant matching in the response. The difference in the peak responses can be attributed to the higher effect of damping in the MCS model. Further observation of the maximum/minimum envelope shows that these responses are

following the path of the mean and deterministic responses. Further, the confidence interval of the response in 10% of uncertainty is not very wide but deviations from the deterministic response are notable. However, the deviations of maximum/minimum envelope and width

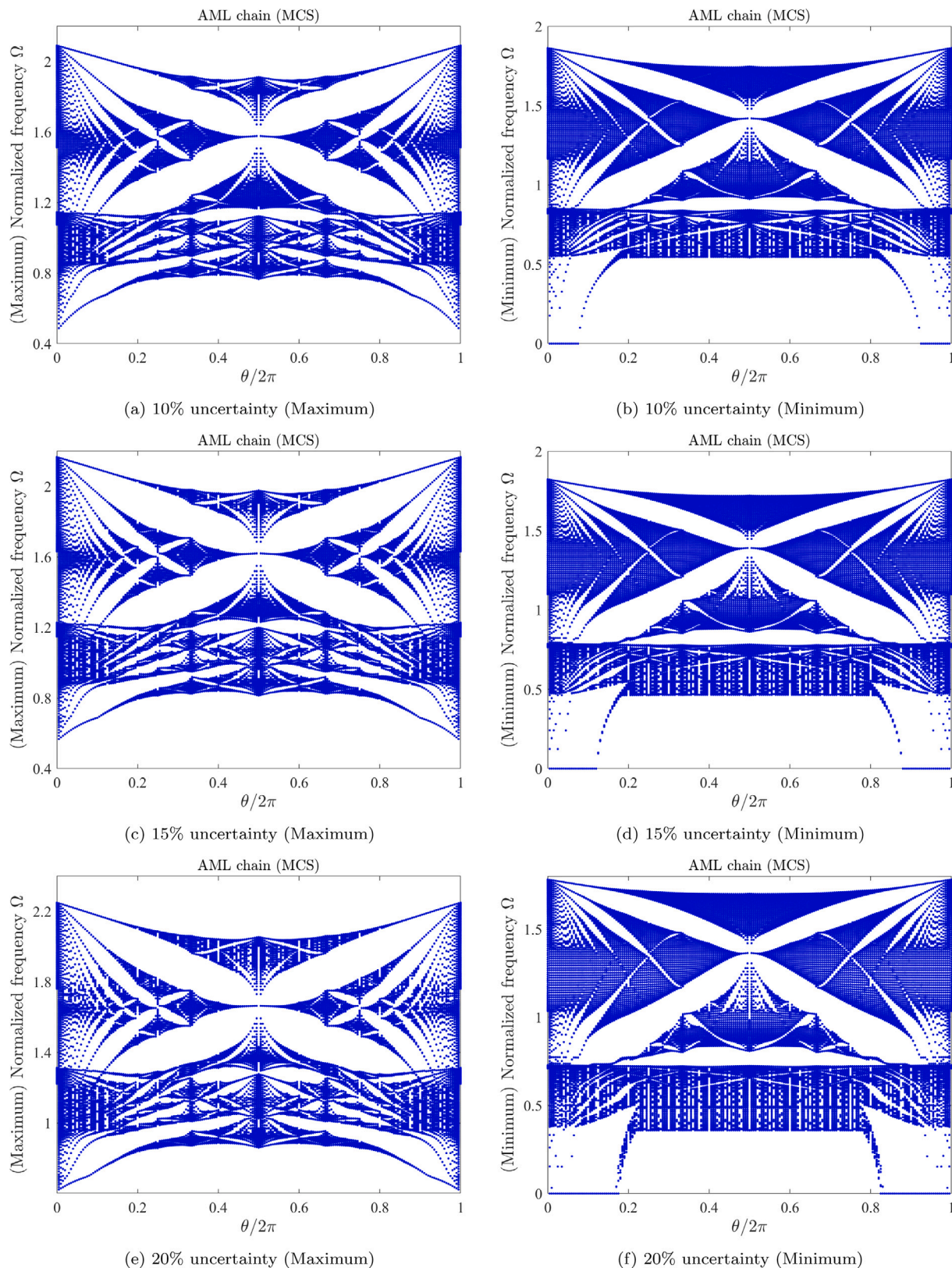
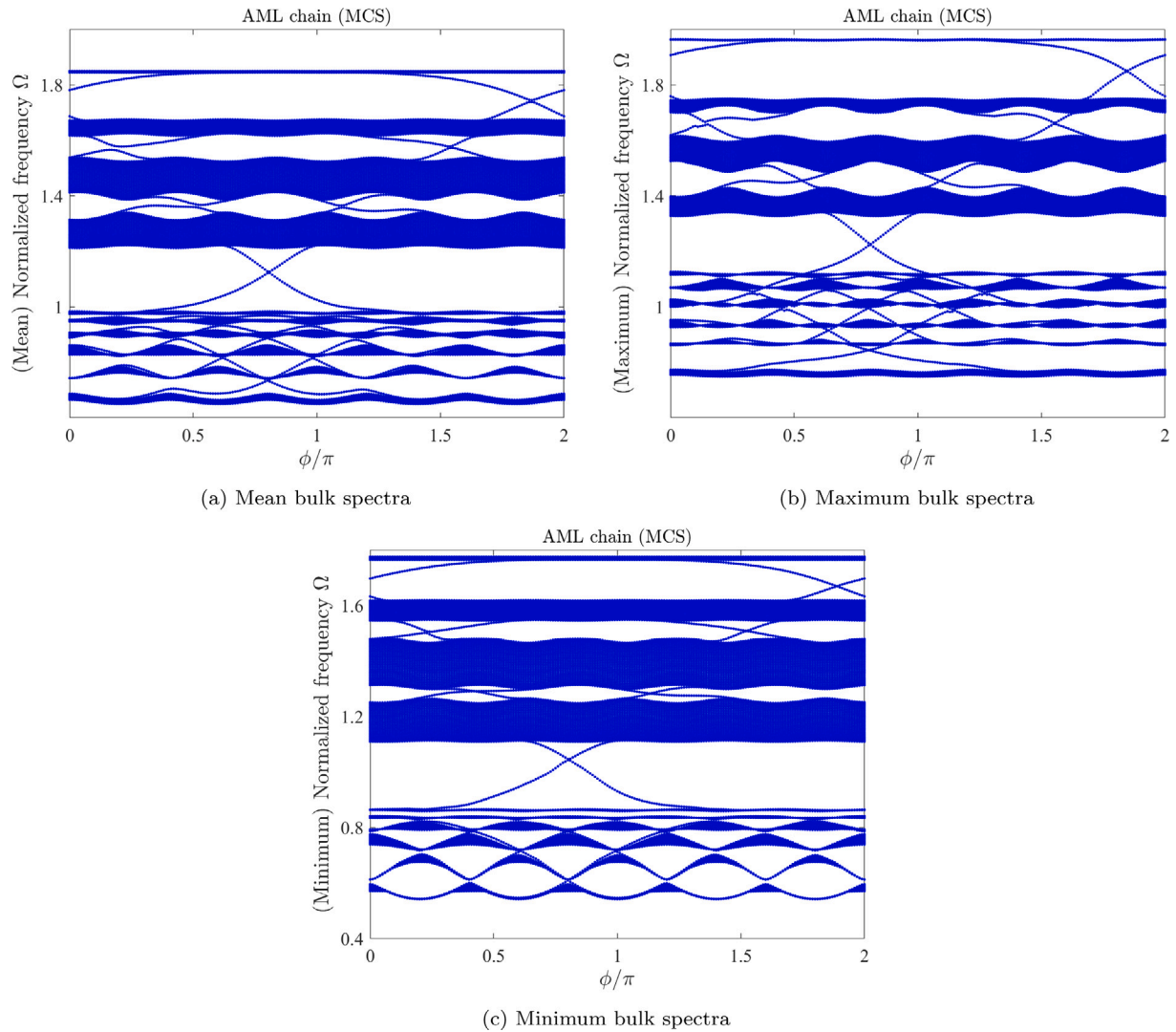


Fig. 7. Maximum and minimum of Hofstadter butterfly spectrum obtained by MCS in the presence of 10%, 15% and 20% uncertainty in the mass, stiffness and inerter parameters.



**Fig. 8.** Statistics of the stochastic bulk spectra and edge states of quasiperiodic AML chain for varying phase  $\phi$  in the presence of 10% uncertainties in the mass, stiffness and inerter parameters. The results have been obtained with the help of 1000 MCS.

of the confidence interval significantly grows for higher percentages of uncertainty. For example, this change is large and visible in the transmission region for 10% uncertainty, however large shifting of the maximum envelope to lower frequency values and amplitude increase can be observed in the vicinity of the zero-frequency gap and for 15% and 20% of uncertainty.

## 5. Conclusion

This study provides a comprehensive analysis of the Hofstadter butterfly spectrum and edge states in 1D quasiperiodic lattices with inerter elements. The two types of lattice configurations were considered, namely the phononic-crystal-like (PCL) and the acoustic-metamaterial-like (AML) chains with local resonators. The main novelty and contribution of this work lies in the fact that the effect of parametric uncertainty and inerter elements in their quasiperiodic setup is investigated for the first time and important conclusions for future design of inerter-based quasiperiodic lattices can be drawn.

The deterministic analysis of Hofstadter butterfly spectrum and edge states in PCL chains with inerters showed shifting of the spectrum to lower frequency values while retaining the main properties of the fractal structure of the butterfly and edge states. However, the same

analysis for the AML chains besides shifting of higher eigenstates to lower frequency values demonstrated a widening of the lower frequency gaps (whose existence is attributed to local resonances) and corresponding edge state frequencies due to the introduction of inertia amplification effect. A similar effect of inerter devices on periodic structures was noticed in the literature.

Finally, parametric uncertainty studies based on Monte Carlo simulations (MCS) and Gaussian process (GP) models illustrated how the statistical variation of parameters affects the butterfly spectrum and edge states in the AML quasiperiodic lattices. It was revealed that GP was capable of effectively capturing the response, compared to that from MCS, with a nominal amount of information (less data). It has been observed that the higher level of uncertainty significantly affects the Hofstadter butterfly and frequency function response, especially the structure of lower frequency gaps.

The study highlights the importance of considering potential uncertainties in analyzing inerter-based quasiperiodic lattices and designing robust wave filters for vibration isolation and energy harvesting applications. This work provides the framework to solve robust design optimization of advanced future application-driven quasiperiodic structural devices.

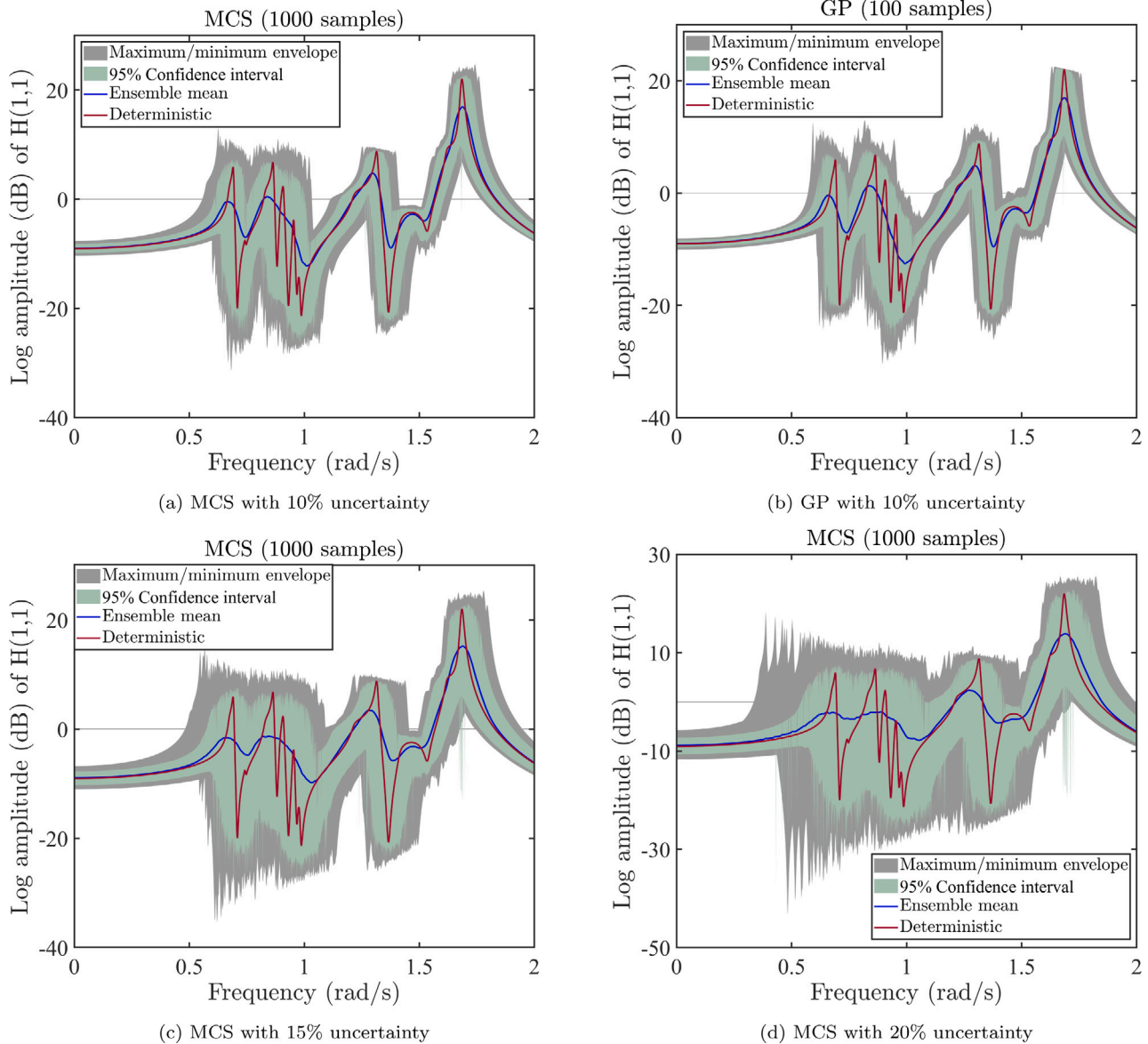


**Fig. 9.** Comparison of the performance of Gaussian process (GP) and Monte Carlo simulations (MCS) in capturing the statistics of direct frequency response function  $H(1,1)$  for 10% uncertainty (see panels (a) and (b)). 100 samples have been employed to train the GP model. Direct frequency response function  $H(1,1)$  bands obtained by MCS in the presence of 15% and 20% uncertainty are given in panels (c) and (d). The FRFs are evaluated assuming 0.5% damping.

#### CRediT authorship contribution statement

**Tanmoy Chatterjee:** Conceptualization, Methodology, Software, Formal analysis, Writing – original draft. **Danilo Karličić:** Conceptualization, Methodology, Formal analysis, Software. **Milan Cajić:** Methodology, Investigation, Visualization, Writing – original draft. **Sondipon Adhikari:** Writing – review & editing, Supervision, Funding acquisition. **Michael I. Friswell:** Writing – review & editing, Supervision, Funding acquisition.

#### Declaration of competing interest

The authors declare that they have no known competing financial interests or personal relationships that could have appeared to influence the work reported in this paper.

#### Data availability

Data will be made available on request.

#### Acknowledgments

TC and MIF gratefully acknowledge the support of the Engineering and Physical Sciences Research Council, UK through the award of a Programme Grant “Digital Twins for Improved Dynamic Design”, grant number EP/R006768. DK acknowledges the support by the Serbian Ministry of Education, Science and Technological Development through the Mathematical Institute of the Serbian Academy of Sciences and Arts. MC and SA acknowledge funding from European Union’s Horizon 2020 research and innovation programme under the Marie Skłodowska-Curie grant agreement No. 896942 (METASINK).

#### Appendix. Gaussian process

The Gaussian process (GP) is a stochastic process which stipulates probability distributions over functions. Originally GP was developed as a spatial interpolation technique in the field of geostatistics [54] and later applied in the dynamics of structures [55]. GP is also known as Kriging. Considering an independent variable  $\mathbf{x} \in \mathbb{R}^d$  and function  $g(\mathbf{x})$

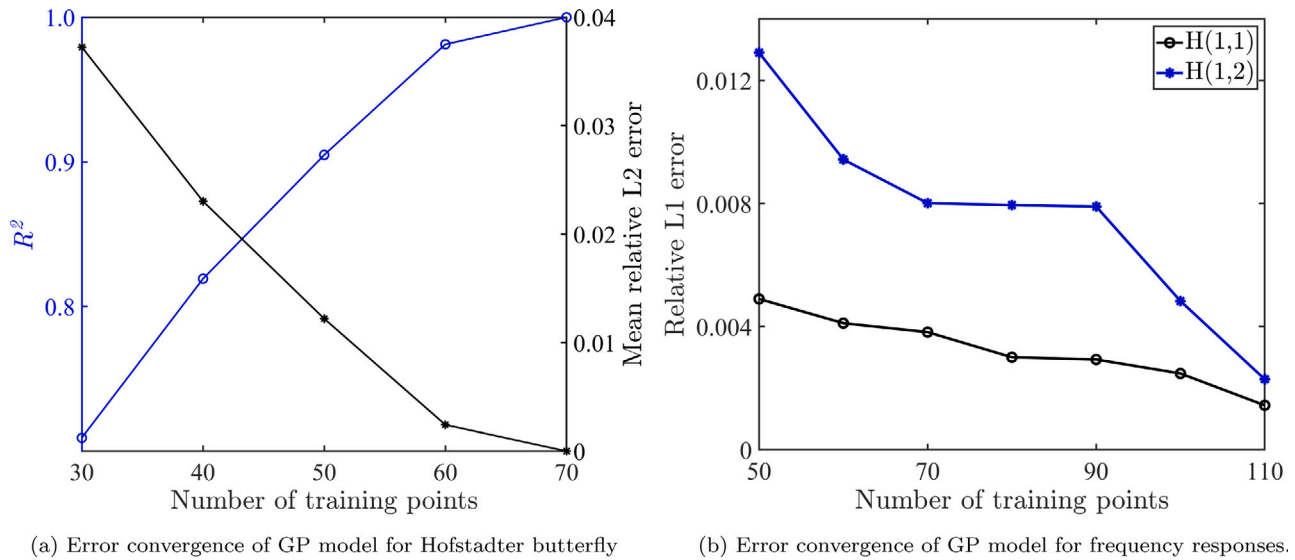


**Fig. 10.** Convergence study to determine the number of samples required for the GP model to adequately capture (a) the dispersion behavior and (b) frequency responses of quasi-periodic lattices. On the basis of the error convergence plots, 50 and 100 training points have been selected for approximating the dispersion behavior and frequency responses, respectively. More points are required for the frequency responses to capture the nonlinear fluctuations owing to low damping (0.5%). For the convergence study, all of the parameters related to mass, stiffness, and inerter properties have been considered to be random with 10% variation.

such that  $g : \mathbb{R}^d \rightarrow \mathbb{R}$ , a GP over  $g(\mathbf{x})$  with mean  $\mu(\mathbf{x})$  and covariance function  $\kappa(\mathbf{x}, \mathbf{x}'; \Theta)$  can be defined as

$$g(\mathbf{x}) \sim GP(\mu(\mathbf{x}), \kappa(\mathbf{x}, \mathbf{x}'; \Theta)),$$

$$\mu(\mathbf{x}) = \mathbb{E}[g(\mathbf{x})] \tag{10}$$

$$\kappa(\mathbf{x}, \mathbf{x}'; \Theta) = \mathbb{E}[(g(\mathbf{x}) - \mu(\mathbf{x}))(g(\mathbf{x}') - \mu(\mathbf{x}'))]$$

where  $\Theta$  denotes the hyperparameters of the covariance function  $\kappa$ . The choice of the covariance function  $\kappa$  allows to incorporate any prior knowledge about  $g(\mathbf{x})$  (for instance, periodicity, linearity, smoothness) and can cope with the approximation of arbitrary complex functions. The covariance function brings in interdependencies between the function value corresponding to different inputs. For instance, the following squared exponential (Gaussian) covariance function is used in this study.

$$\kappa(\mathbf{x}, \mathbf{x}') = \sigma_g^2 \exp \left[ - \sum_{i=1}^d \frac{(x(i) - x'(i))^2}{2r_i^2} \right] \tag{11}$$

where  $\{\sigma_g, r_1, \dots, r_d\} = \Theta$  are the hyperparameters of the covariance function.

One perspective of viewing GP is the function-space mapping describing the input–output relationship [56]. As opposed to conventional modeling techniques which employ fitting a parameterized mathematical form to map the input–output functional space, a GP does not assume any explicit form, and instead holds a prior belief (in the form of the mean and covariance function) onto the space of model (response) functions. Thus, GPs can be classified as a 'non-parametric' model as the number of parameters in the model is governed by the number of available data points.

The most general form of GP, called Universal Kriging, is used in this study [57]. This can be represented by second-order polynomial trend functions and can be expressed as

$$\mathbf{y}(\mathbf{x}) = \sum_{j=1}^p \beta_j \mathbf{f}_j(\mathbf{x}) + \mathbf{z}(\mathbf{x}) \tag{12}$$

where  $\beta = \{\beta_j, j = 1, \dots, p\}$  is the vector of unknown coefficients and  $\mathbf{F} = \{\mathbf{f}_j, j = 1, \dots, p\}$  is the matrix of polynomial basis functions.  $\mathbf{z}(\mathbf{x})$  is the GP with zero mean and autocovariance  $\text{cov}[\mathbf{z}(\mathbf{x}), \mathbf{z}(\mathbf{x}')] = \sigma^2 \mathbf{R}(\mathbf{x}, \mathbf{x}')$ , where  $\sigma^2$  is the process variance and  $\mathbf{R}(\mathbf{x}, \mathbf{x}')$  is the autocorrelation function.

The parameters  $\beta$  and  $\sigma^2$  can be estimated by the maximum likelihood estimate (MLE) defined by the following optimization problem under the assumption that the noise  $\mathbf{z} = \mathbf{y} - \mathbf{F}\beta$  is a correlated Gaussian vector

$$(\hat{\beta}, \hat{\sigma}^2) = \arg \max_{\beta, \sigma^2} \mathbf{L}(\beta, \sigma^2 | \mathbf{y})$$

$$= \frac{1}{((2\pi\sigma^2)^n \det \mathbf{R})^2} \exp \left[ - \frac{1}{2\sigma^2} (\mathbf{y} - \mathbf{F}\beta)^T \mathbf{R}^{-1} (\mathbf{y} - \mathbf{F}\beta) \right] \tag{13}$$

Upon solving Eq. (13), the estimates  $(\hat{\beta}, \hat{\sigma}^2)$  can be obtained as

$$\hat{\beta} = (\mathbf{F}^T \mathbf{R}^{-1} \mathbf{F})^{-1} \mathbf{F}^T \mathbf{R}^{-1} \mathbf{y} \tag{14}$$

$$\hat{\sigma}^2 = \frac{1}{n} (\mathbf{y} - \mathbf{F}\hat{\beta})^T \mathbf{R}^{-1} (\mathbf{y} - \mathbf{F}\hat{\beta}) \tag{15}$$

where  $\mathbf{y}$  represents the model response such that  $\mathbf{y} = \{y_1, \dots, y_n\}^T$ .

The prediction response for a test point requires three conditions to be satisfied, which are linearity in terms of the observed data, unbiasedness and minimal variance. The prediction mean and variance by GP can be obtained as

$$\mu_{\hat{\mathbf{y}}}(\mathbf{x}) = \mathbf{F}^T \hat{\beta} + \mathbf{r}^T \mathbf{R}^{-1} (\mathbf{y} - \mathbf{F}\hat{\beta}) \tag{16}$$

$$\sigma_{\hat{\mathbf{y}}}^2(\mathbf{x}) = \hat{\sigma}^2 [1 - \mathbf{r}^T \mathbf{R}^{-1} \mathbf{r} + \mathbf{u}^T (\mathbf{F}^T \mathbf{R}^{-1} \mathbf{F})^{-1} \mathbf{u}] \tag{17}$$

where  $\mathbf{u} = \mathbf{F}^T \mathbf{R}^{-1} \mathbf{r} - \mathbf{R}$  and  $\mathbf{r}$  is the autocorrelation between the unknown point  $\mathbf{x}$  and each point of the observed data set.

Some unique features of the above formulation are: (i) The prediction is exact at the training points and the associated variance is zero. (ii) It is asymptotically zero which means that as the size of the observed data set increases, the overall variance of the process decreases. (iii) The prediction at a given point is considered as a realization of a Gaussian random variable. Thus, it is possible to derive confidence bounds on the prediction. The variance information is often used as an error measure of the epistemic uncertainty of the meta-model due to sparsity of data. This feature has led to the development of adaptive error based sampling schemes for improving the accuracy of the meta-model [58,59].

## References

- [1] Süsstrunk R, Huber SD. Observation of phononic helical edge states in a mechanical topological insulator. *Science* 2015;349(6243):47–50.
- [2] Bertoldi K, Vitelli V, Christensen J, Van Hecke M. Flexible mechanical metamaterials. *Nat Rev Mater* 2017;2(11):1–11.
- [3] Bansil A, Lin H, Das T. Colloquium: Topological band theory. *Rev Modern Phys* 2016;88(2):021004.
- [4] Yang Z, Gao F, Shi X, Lin X, Gao Z, Chong Y, et al. Topological acoustics. *Phys Rev Lett* 2015;114(11):114301.
- [5] Fleury R, Khanikaev AB, Alu A. Floquet topological insulators for sound. *Nature Commun* 2016;7(1):1–11.
- [6] Mousavi SH, Khanikaev AB, Wang Z. Topologically protected elastic waves in phononic metamaterials. *Nature Commun* 2015;6(1):1–7.
- [7] Li L, Xu Z, Chen S. Topological phases of generalized Su–Schrieffer–Heeger models. *Phys Rev B* 2014;89(8):085111.
- [8] Li S, Zhao D, Niu H, Zhu X, Zang J. Observation of elastic topological states in soft materials. *Nature Commun* 2018;9(1):1–9.
- [9] Ma G, Xiao M, Chan CT. Topological phases in acoustic and mechanical systems. *Nat Rev Phys* 2019;1(4):281–94.
- [10] Wang J, Huang Y, Chen W. Tailoring edge and interface states in topological metastructures exhibiting the acoustic valley Hall effect. *Sci China Phys Mech Astron* 2020;63(2):1–11.
- [11] Gao N, Qu S, Si L, Wang J, Chen W. Broadband topological valley transport of elastic wave in reconfigurable phononic crystal plate. *Appl Phys Lett* 2021;118(6):063502.
- [12] Xiao M, Ma G, Yang Z, Sheng P, Zhang Z, Chan CT. Geometric phase and band inversion in periodic acoustic systems. *Nat Phys* 2015;11(3):240–4.
- [13] Chaunsali R, Kim E, Thakkar A, Kevrekidis PG, Yang J. Demonstrating an in situ topological band transition in cylindrical granular chains. *Phys Rev Lett* 2017;119(2):024301.
- [14] Zhou W, Lim C, et al. Topological edge modeling and localization of protected interface modes in 1D phononic crystals for longitudinal and bending elastic waves. *Int J Mech Sci* 2019;159:359–72.
- [15] Zhao D, Xiao M, Ling CW, Chan CT, Fung KH. Topological interface modes in local resonant acoustic systems. *Phys Rev B* 2018;98(1):014110.
- [16] Yao L, Zhang D, Xu K, Dong L, Chen X. Topological phononic crystal plates with locally resonant elastic wave systems. *Appl Acoust* 2021;177:107931.
- [17] Pal RK, Vila J, Leamy M, Ruzzene M. Amplitude-dependent topological edge states in nonlinear phononic lattices. *Phys Rev E* 2018;97(3):032209.
- [18] Darabi A, Leamy MJ. Tunable nonlinear topological insulator for acoustic waves. *Phys Rev A* 2019;102(4):044030.
- [19] Zhou D, Rocklin D, Leamy M, Yao Y. Topological invariant and anomalous edge states of strongly nonlinear systems. 2020, arXiv preprint arXiv:2012.14103.
- [20] Wang H, Liu D, Fang W, Lin S, Liu Y, Liang Y. Tunable topological interface states in one-dimensional extended granular crystals. *Int J Mech Sci* 2020;176:105549.
- [21] Tempelman JR, Matlack KH, Vakakis AF. Topological protection in a strongly nonlinear interface lattice. *Phys Rev B* 2021;104(17):174306.
- [22] Aubry S, André G. Analyticity breaking and Anderson localization in incommensurate lattices. *Ann Isr Phys Soc* 1980;3(133):18.
- [23] Apigo DJ, Qian K, Prodan C, Prodan E. Topological edge modes by smart patterning. *Phys Rev Mater* 2018;2(12):124203.
- [24] Rosa MI, Leamy MJ, Ruzzene M. Amplitude-dependent edge states and discrete breathers in nonlinear modulated phononic lattices. 2022, arXiv preprint arXiv:2201.05526.
- [25] Prodan E, Schulz-Baldes H. Bulk and boundary invariants for complex topological insulators. *K* 2016.
- [26] Cheng W, Apigo D, Dobiszewski K, Prodan E, Prodan C. Observation of topological edge modes in a quasi-periodic acoustic waveguide. In: APS march meeting abstracts, vol. 2019. 2019, p. A03–008.
- [27] Ni X, Chen K, Weiner M, Apigo DJ, Prodan C, Alu A, et al. Observation of Hofstadter butterfly and topological edge states in reconfigurable quasi-periodic acoustic crystals. *Commun Phys* 2019;2(1):1–7.
- [28] Xia Y, Erturk A, Ruzzene M. Topological edge states in quasiperiodic locally resonant metastructures. *Phys Rev A* 2020;103(1):014023.
- [29] Rosa MI, Guo Y, Ruzzene M. Exploring topology of 1D quasiperiodic metastructures through modulated LEGO resonators. *Appl Phys Lett* 2021;118(13):131901.
- [30] Beli D, Rosa MIN, Marqui Jr CD, Ruzzene M. Wave beaming and diffraction in quasicrystalline elastic metamaterial plates. 2022, arXiv preprint arXiv:2201.12270.
- [31] Beli D, Rosa MIN, De Marqui Jr C, Ruzzene M. Mechanics and dynamics of two-dimensional quasicrystalline composites. *Extreme Mech Lett* 2021;44:101220.
- [32] Kuhnert WM, Gonçalves PJP, Ledezma-Ramirez DF, Brennan MJ. Inerter-like devices used for vibration isolation: a historical perspective. *J Franklin Inst B* 2021;358(1):1070–86.
- [33] Smith MC. The inerter: a retrospective. *Annu Rev Control Robot Auton Syst* 2020;3:361–91.
- [34] Liu X, Jiang JZ, Titurus B, Harrison A. Model identification methodology for fluid-based inerters. *Mech Syst Signal Process* 2018;106:479–94.
- [35] Wagg DJ. A review of the mechanical inerter: historical context, physical realisations and nonlinear applications. *Nonlinear Dynam* 2021;1–22.
- [36] Mi Y, Lu Z, Yu X. Acoustic inerter: Ultra-low frequency sound attenuation in a duct. *J Acoust Soc Am* 2020;148(1):EL27–32.
- [37] Kulkarni PP, Manimala JM. Longitudinal elastic wave propagation characteristics of inertant acoustic metamaterials. *J Appl Phys* 2016;119(24):245101.
- [38] Mu D, Shu H, Zhao L, An S. A review of research on seismic metamaterials. *Adv Energy Mater* 2020;22(4):1901148.
- [39] Fang X, Chuang K-C, Jin X, Huang Z. Band-gap properties of elastic metamaterials with inerter-based dynamic vibration absorbers. *J Appl Mech* 2018;85(7):071010.
- [40] Al Ba'ba'a H, DePaauw D, Singh T, Nohu M. Dispersion transitions and pole-zero characteristics of finite inertially amplified acoustic metamaterials. *J Appl Phys* 2018;123(10):105106.
- [41] Al Ba'ba'a H, Zhu X, Wang Q. Enabling novel dispersion and topological characteristics in mechanical lattices via stable negative inertial coupling. *Proc R Soc A* 2021;477(2252):20200820.
- [42] Henneberg J, Nieto JG, Sepahvand K, Gerlach A, Cebulla H, Marburg S. Periodically arranged acoustic metamaterial in industrial applications: The need for uncertainty quantification. *Appl Acoust* 2020;157:107026.
- [43] Al Ba'ba'a H, Nandi S, Singh T, Nohu M. Uncertainty quantification of tunable elastic metamaterials using polynomial chaos. *J Appl Phys* 2020;127(1):015102.
- [44] Chatterjee T, Karličić D, Adhikari S, Friswell MI. Wave propagation in randomly parameterized 2D lattices via machine learning. *Compos Struct* 2021;275:114386.
- [45] Cajić M, Karličić D, Christensen J, Adhikari S. Tunable topological interface states in one-dimensional inerter-based locally resonant lattices with damping. *J Sound Vib* 2023;542:117326.
- [46] Smith MC. Synthesis of mechanical networks: the inerter. *IEEE Trans Automat Control* 2002;47(10):1648–62.
- [47] Shen W, Long Z, Cai L, Niyitangamahoro A, Zhu H, Li Y, et al. An inerter-based electromagnetic damper for civil structures: Modeling, testing, and seismic performance. *Mech Syst Signal Process* 2022;173:109070.
- [48] De Domenico D, Deastra P, Ricciardi G, Sims ND, Wagg DJ. Novel fluid inerter based tuned mass dampers for optimised structural control of base-isolated buildings. *J Franklin Inst B* 2019;356(14):7626–49.
- [49] Aladwani A, Mohammed A, Nohu M. Tunable dissipation in elastic metamaterials via methodic reconfiguration of inertant mechanical networks. *Meccanica* 2022;57(6):1337–52.
- [50] Van Damme B, Hannema G, Sales Souza L, Weisse B, Tallarico D, Bergamini A. Inherent non-linear damping in resonators with inertia amplification. *Appl Phys Lett* 2021;119(6):061901.
- [51] Russillo AF, Failla G, Alotta G. Ultra-wide low-frequency band gap in locally-resonant plates with tunable inerter-based resonators. *Appl Math Model* 2022;106:682–95.
- [52] Pal RK, Rosa MI, Ruzzene M. Topological bands and localized vibration modes in quasiperiodic beams. *New J Phys* 2019;21(9):093017.
- [53] Yilmaz C, Hulbert GM, Kikuchi N. Phononic band gaps induced by inertial amplification in periodic media. *Phys Rev B* 2007;76(5):054309.
- [54] Krige DG. A statistical approach to some basic mine valuation problems on the witwatersrand. *J Chem Metall Min Soc S Afr* 1951;52(6):119–39.
- [55] Chatterjee T, Adhikari S, Friswell MI. Uncertainty propagation in dynamic sub-structuring by model reduction integrated domain decomposition. *Comput Methods Appl Mech Engrg* 2020;366:113060.
- [56] Rasmussen CE, Williams CKI. Gaussian processes for machine learning. Cambridge, Massachusetts London, England: The MIT Press; 2006.
- [57] Lophaven S, Nielson H, Sondergaard J. DACE A MATLAB kriging toolbox. Tech. rep. IMM-TR-2002-12, Technical University of Denmark; 2002.
- [58] Chatterjee T, Chowdhury R. h – p adaptive model based approximation of moment free sensitivity indices. *Comput Methods Appl Mech Engrg* 2018;332:572–99.
- [59] Chatterjee T, Chowdhury R. Adaptive bilevel approximation technique for multi-objective evolutionary optimization. *J Comput Civ Eng* 2017;31(3):04016071.